Dispersion-Induced Power Penalties in Millimeter-Wave Signal Transmission Using Multisection DBR Semiconductor Laser

Christina Lim, *Member, IEEE*, Dalma Novak, *Member, IEEE*, Ampalavanapillai Nirmalathas, *Member, IEEE*, and Graham H. Smith, *Member, IEEE*

***Abstract*—In this paper, we present a simple analytical model to characterize the effect of fiber chromatic dispersion when using a multisection distributed-Bragg reflector (DBR) semiconductor laser as a millimeter-wave optical transmitter in a millimeter-wave fiber-radio system. We characterize the dispersion penalty of the laser as a function of the laser operating conditions and establish that the penalty is dependent on the distribution of optical power among the modes in the laser output. This, in turn, is dependent on the spectrum-filtering property of the laser DBR section and the gain profile of the laser. In addition to the dispersion penalty, the stability of the generated millimeter-wave carrier from the multisection laser is investigated, including the detected RF power and resulting phase noise. We establish that a compromise must be made when finding the optimum bias condition of the laser, which provides minimum dispersion penalty, maximum received RF power, and minimum phase noise of the generated millimeter-wave carrier.**

***Index Terms*—Fixed wireless access networks, millimeter-wave communications, millimeter-wave technology, mode locked, semiconductor lasers.**

I. Introduction

MILLIMETER-WAVE radio access networks are being proposed for the future distribution of broad-band services [1]. The millimeter-wave frequency band offers large transmission bandwidth and also overcomes spectral congestion at lower frequencies. In addition, millimeter-wave radio systems enable efficient frequency reuse due to the limited propagation distances at these frequencies. Optical fiber with its low loss, large bandwidth, and immunity to electromagnetic interference characteristics serves as an ideal transmission medium for the distribution of the millimeter-wave radio signals. In the typical architecture of a millimeter-wave wireless access system with optical fiber backhaul, the radio signals are generated at a central location before distribution via fiber to a number of remote antenna base stations for wireless distribution. Such an architecture moves the radio signal processing and routing functions to the central office, allowing the remote base stations to share resources, thereby simplifying the network architecture. The requirement for more base stations due to the limited wireless coverage area at millimeter-wave frequencies also demands the installation of functionally simple and compact base stations. This can be achieved by transmitting the radio signals at the required millimeter-wave frequency, which reduces the complexity of the electronics required at the base stations, since millimeter-wave up- or down-converting mixers and local oscillators are not required there [2].

The distribution of millimeter-wave signals in a fiber-radio system requires optical millimeter-wave sources both at the central office and base station. To date, a number of techniques for the generation of millimeter-wave modulated optical carriers for downstream data transmission in fiber-wireless systems have been reported and demonstrated [3]–[10]. These methods include optical heterodyne [4], [9] and self-heterodyne [3] techniques, resonantly enhanced semiconductor lasers [6], [7], and pulsed lasers [10]. However, few techniques have been reported for data transmission in the upstream direction in a full-duplex fiber-radio access network. Thus far, upstream data transmission has been accomplished by first down-converting the millimeter-wave wireless signals arriving at the base station from the customer to a lower IF, before transmission over fiber back to the central office [3]. However, this approach leads to more equipment hardware at the base station due to the need for a down-converting mixer and low phase-noise millimeter-wave local oscillator. Recently, we demonstrated for the first time, upstream data transmission at millimeter-wave frequencies by incorporating a multisection distributed Bragg reflector (DBR) laser at the antenna base station [11]. Our technique involved the direct modulation of the multisection laser with the uplink millimeter-wave wireless signals, before transmission of the millimeter-wave modulated optical signals over fiber back to the central office. Such a technique enables a simple antenna base-station architecture to be implemented. We demonstrated the transmission of 51.8 Mb/s of data at 37 GHz in a fiber-radio network incorporating a 5-m wireless link and 40 km of optical fiber, with successful recovery of the data at the central office [11]. In our previous investigation, we also observed that the effect of fiber chromatic dispersion on the transmission of data at millimeter-wave frequencies using the multisection laser is dependent on the optical power distribution in the lasing modes [11].

Manuscript received August 10, 1999.

C. Lim, D. Novak, and A. Nirmalathas are with Australian Photonics CRC, Photonics Research Laboratory, Department of Electrical Engineering, The University of Melbourne, Parkville 3052, Vic., Australia.

G. H. Smith is with the Optical Enterprise Networks Research Group, Bell Laboratories, Lucent Technologies, Holmdel, NJ 07733 USA.

Publisher Item Identifier S 0018-9480(01)01068-7.

Fiber chromatic dispersion has been shown to have a significant effect in direct-detection optical communication systems, which severely limits the fiber-link transmission distance [12]. This effect is even more pronounced in millimeter-wave fiber links [13]–[15]. With an external intensity modulation scheme, RF modulation of the optical carrier produces many optical modulation sidebands, which are spaced at the RF frequency on both sides of the optical carrier. However, under a relatively low modulation index, the optical spectrum is reduced to a carrier with two modulation sidebands. When this modulated optical signal propagates over fiber, each spectral component experiences different phase shifts due to fiber chromatic dispersion. At the optical receiver, the phase shifts cause relative phase differences in the two RF beat signals, which results in a power penalty in the composite RF signal [13]–[15]. As a result, complete cancellation of the RF power can occur when the phase difference between the two beat signals is equal to 180°. This effect is dependent on the modulation frequency, the fiber dispersion parameter, and the fiber transmission length [13]. For example, at a modulation frequency of 38 GHz, the RF signal suffers a 3-dB power loss after traversing a fiber distance of less than 1.2 km [14].

In this paper, we further investigate and present a detailed analysis of the dispersion-induced RF power penalties when transmitting data at millimeter-wave frequencies via direct modulation of a multisection DBR semiconductor laser. In particular, we investigate how the distribution of optical power amongst the lasing modes affects the dispersion power penalty and consider the influence of the DBR section in shaping the laser optical spectrum. In doing so, we develop a simple analytical model to simulate the dispersion-induced carrier power penalty when directly modulating the multisection laser. Our analysis shows that the effect of fiber dispersion can be accurately modeled using a four optical mode model for the multisection laser. In addition, measurements indicate that the efficiency of the laser as a millimeter-wave signal transmitter is dependent on the laser locking condition. These results provide a guideline for the design of the DBR region in such lasers in order to optimize the device to achieve the optical generation of millimeter-wave signals that exhibit low phase noise with maximum detected RF power and, when transmitted over fiber, suffer minimal effects of fiber chromatic dispersion.

This paper is organized as follows. Section II provides a description of the analytical model for simulating the dispersion-induced power penalties in the multisection laser. Section III describes the experimental and theoretical characterization of the dispersion-induced power penalty, while Section IV focuses on other factors, such as the detected RF power and the phase noise of the beat signal, which also influence the efficiency of the laser as a millimeter-wave transmitter. Finally, conclusions are presented in Section V.

II. Chromatic Dispersion Model for Multisection Laser

In this section, we model the effect of fiber chromatic dispersion on the millimeter-wave optical carriers generated by the multisection DBR semiconductor laser. The multisection laser consists of two gain sections, a DBR section, a phase control (PC) section, and a saturable absorber (SA) region [16]. Under continuous wave (CW) operation, the output from the laser comprises several modes with frequency spacing determined by the cavity length (typically 1.1 mm). When the laser is biased at certain conditions, the laser modes can be passively mode locked to generate a pulse train at the repetition frequency, which is equal to the mode-spacing frequency (approximately 37 GHz) [11]. Under such conditions, an ultra-stable low-noise millimeter-wave optical carrier can be generated from the laser by injecting a 37-GHz electrical signal into the SA of the device (hybrid mode locking) [17]. Fig. 1(a) and (b) shows the measured optical spectra of the multisection laser with an RF carrier at 37 GHz applied to the device. In Fig. 1(a), the gain sections of the laser were biased at dc currents of 42 and 81.4 mA with a short-circuit termination at the SA region, while Fig. 1(b) shows the spectrum with gain currents of 42 and 58.8 mA, and an open-circuit termination at the SA. The DBR and PC regions were left with open-circuit terminations. The optical spectrum of the multisection laser was measured using an optical spectrum analyzer with a resolution bandwidth of 0.1 nm. Fig. 1(a) shows that the power distribution amongst the laser modes is asymmetric when a short circuit is connected to the SA. In addition, two more modes are present in the laser output compared to when the SA is left with an open-circuit termination. This indicates that when the SA is terminated with a short-circuit, the absorber recovery time is reduced, which enhances the mode-locking process within the multisection laser [18].

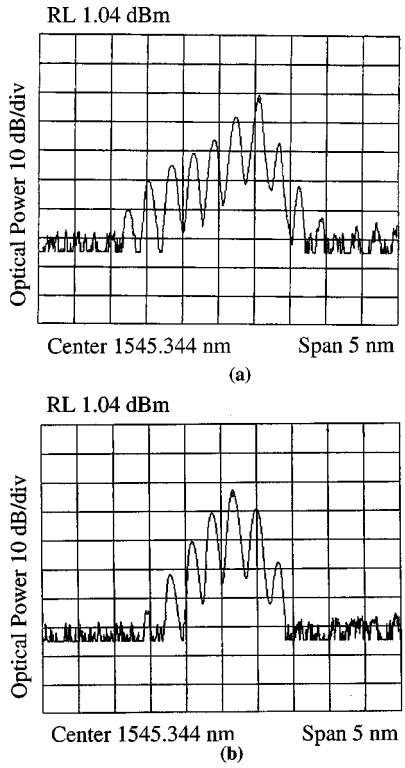

Fig. 1. Measured optical spectra of the multisection laser when biased with: (a) $I_{g1} = 42$ mA, $I_{g2} = 81.4$ mA and the SA with a short-circuit termination and (b) $I_{g1} = 42$ mA, $I_{g2} = 58.8$ mA and the SA with an open-circuit termination.

The DBR section of the multisection laser has a specific reflectivity profile, which, together with the gain profile, deter-

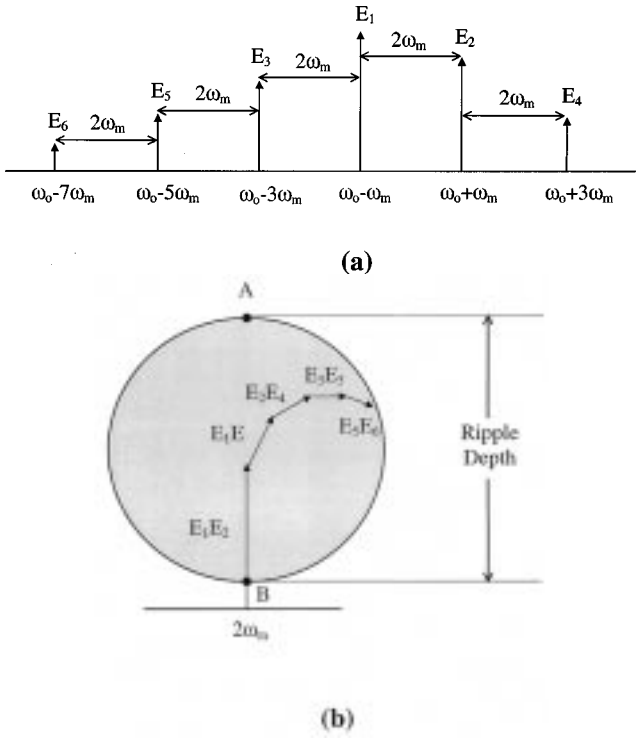

Fig. 2. (a) Schematic diagram of the optical spectrum from the multisection laser. (b) Phasor diagram showing the vectorial addition of the detected RF beat signal with frequency $2\omega_m$.

mines the lasing modes of the multisection laser [16]. As the gain profile is broader in bandwidth compared to the reflectivity profile, the number of modes and optical power distribution amongst the modes in the laser output will be largely dependent on the strength of the DBR reflectivity [16], [19]. The cavity modes that fall within the passband of the DBR profile will be enhanced while those that fall outside the passband will be suppressed. If the reflectivity of the DBR section is weak, the laser operates in a similar manner to a Fabry–Perot cavity with the end mirrors providing the feedback [20]. However, when the laser has a strong DBR reflectivity profile, the DBR section acts as a narrow-band filter [20].

Both optical spectra in Fig. 1 show a laser output, which is multimoded with at least six dominant modes. When this optical signal is incident on a photodetector (PD), a number of beat signals at the laser repetition frequency will be generated. When the optical signal is transported over optical fiber, however, these modes will experience different phase shifts due to fiber chromatic dispersion. Depending on the relative phase differences in the resulting beat signals at the PD, this may result in a loss in the detected RF power of the composite millimeter-wave beat signal. This can be visualized using Fig. 2, which shows a schematic diagram of the laser spectrum [see Fig. 2(a)] and a phasor diagram of the composite beat signals [see Fig. 2(b)]. The optical spectrum shown in Fig. 2(a) consists of six modes labeled as electric fields E_1–E_6 with varying amplitudes representing the different optical power in each mode. The laser spectrum is centered at optical radio frequency ω_0, with the mode separation frequency given by $2\omega_m$. When the signal in Fig. 2(a) is detected, five beat signal components at frequency $2\omega_m$ will be generated with varying amplitude and phase, as depicted in Fig. 2(b). In Fig. 2(b), each beat signal is shown as a phasor with length determined by the detected RF power, which is proportional to the square of the product of the electric fields associated with the two modes, which mix together. These beat signal phasors then add together to give a resultant RF signal at $2\omega_m$. Depending on the dispersion-induced phase shift, when all the beat signal components add in phase (as indicated by point A), the detected RF power will be a maximum, while a minimum RF power occurs at point B. The RF power difference between points A and B, therefore, defines a fiber dispersion-induced RF power loss penalty [11].

The schematic of the analytical model for simulating the dispersion-induced RF power penalty in the multisection laser is shown in Fig. 3. The input parameters for the model are the measured powers of the six dominant modes in the laser spectrum with varying amplitudes labeled E_1–E_6. As the optical modes of the laser under hybrid mode locking are locked in phase, these modes have a fixed phase relationship with each other. Each optical mode within the passband of the DBR reflectivity profile has a relative initial phase, which is determined by the phase response of the DBR reflectivity profile and governed by the equation shown in Fig. 3 [20], [21]. Amplitude response is already included in the power distribution as the measured optical power of each mode from the input.

In order to determine the effect of fiber dispersion on the transmission of the multisection laser signals, the optical fiber link was modeled as a low-pass filter with negligible attenuation [22]. For simplicity, noise processes and polarization effects in the fiber were neglected in the dispersion model. When the laser signal is transported over fiber, the effect of chromatic dispersion on each of the propagating laser modes can be modeled by a constant phase delay in the optical field relative to ω_o. The phase delay φ, after propagation through L km of fiber, is given by the equation shown in Fig. 3 [13]. The resulting photocurrents of the beat signal components are proportional to the square of the optical field. At the end of the optical link, each mode will beat with all others in the PD to generate a series of RF frequencies in the RF spectrum of the PD current. Due to the finite response of the PD, all higher order RF carriers will be suppressed, leaving only the RF signals that are centered at the fundamental repetition frequency of the laser, i.e., $2\omega_m$. Vector addition of these beat components generates a composite millimeter-wave carrier, which is dependent on the relative phases of the beat signals.

Taking $D = 17$ ps $\cdot$ nm $\cdot$ km for a standard single-mode fiber (SMF), $2f_m = 37$ GHz and $\lambda_0 = 1545.6$ nm, the detected RF power can be plotted as a function of fiber length. Figs. 4 and 5 show the theoretical plots (solid lines) of detected RF power at 37 GHz from the multisection laser corresponding to the measured optical spectra shown in Fig. 1(a) and (b), respectively. The normalized RF power is defined as the detected RF power at L km of fiber transmission length relative to the RF power measured at 0 km. The measured amplitudes of each of the optical modes in the laser optical spectra, as shown in Fig. 1, were used as values for E_1–E_6.

The experimental setup for the measurement of a dispersion-induced RF power penalty when transporting the multisection

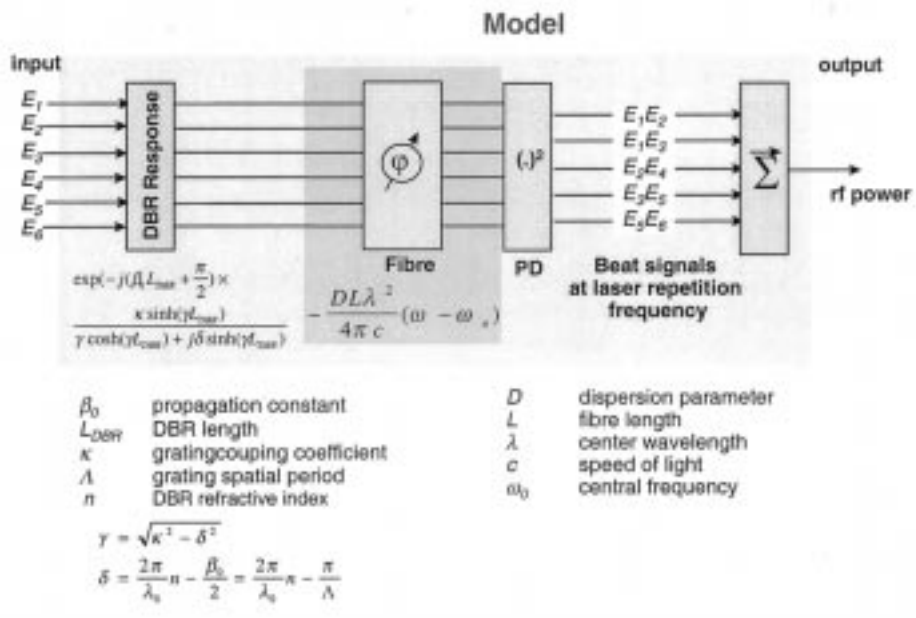

Fig. 3. Schematic diagram of analytical model to predict dispersion-induced RF power penalties in a multisection laser.

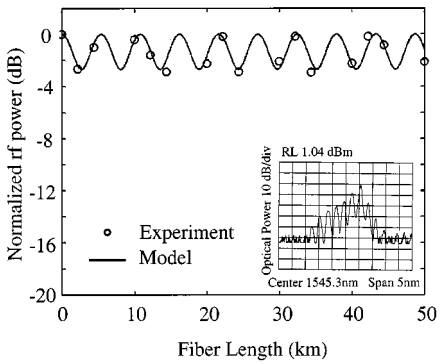

Fig. 4. Measured and predicted dispersion-induced RF power penalty in multisection laser biased at $I_{g1} = 42$ mA, $I_{g2} = 81$ mA with a short-circuit at the SA (inset shows the measured laser optical spectrum at the bias point).

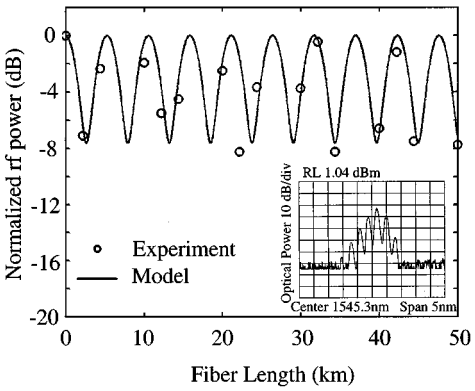

Fig. 5. Measured and predicted dispersion-induced RF power penalty in multisection laser biased at $I_{g1} = 42$ mA, $I_{g2} = 58.8$ mA with open circuit at the SA (inset shows the measured laser optical spectrum at the bias point).

laser signal over optical fiber is shown in Fig. 6. A tunable laser set at the center frequency of the multisection laser and an erbium-doped fiber amplifier (EDFA) were first used to calibrate for any losses due to fiber attenuation and connector losses. An optical bandpass filter (BPF) after the EDFA removes excess amplified spontaneous emission (ASE) noise. An external RF carrier with a frequency corresponding to the laser repetition frequency of 37 GHz was then injected into the multisection laser. The signal was transported over L km of a SMF and the detected RF power was measured using a 40-GHz RF spectrum analyzer in conjunction with a 45-GHz PD (responsivity $\approx$0.3 A/W) and a low-noise millimeter-wave amplifier (LNA). Figs. 4 and 5 show the normalized measured detected RF power at 37 GHz as a function of fiber length for the same laser bias conditions given in Fig. 1. The ripple depth of the dispersion-induced RF power penalty is defined as the difference between the maximum and minimum detected RF powers. It is evident from Figs. 4 and 5 that the dispersion penalty differs for the two bias conditions of the multisection laser, with a dispersion ripple of 2.8 dB in Fig. 4 increasing to 7.5 dB in Fig. 5. This difference will be the subject of investigation in Section III.

The theoretical plots derived from our model also show good agreement with the experimental results. It should be noted that, in the model, we assume that the dispersion parameter D is constant throughout the entire length of the fiber. However, in the experiment, each length of fiber used has slightly different D parameters, which result in the small discrepancy between experimental and theoretical results. In addition, in the model developed here, the effect of decorrelation of the optical modes as the signal propagates through fiber was not taken into account [15]. It has been shown that fiber dispersion also increases the phase noise of the detected RF signal due to mode decorrelation, which can further limit the fiber transmission length, particularly when higher order modulation schemes are used [15]. Nevertheless, the close fit of the experimental and theoretical results confirms that the model is capable of predicting the effect of fiber dispersion when the optical output spectrum of the multisection laser is known.

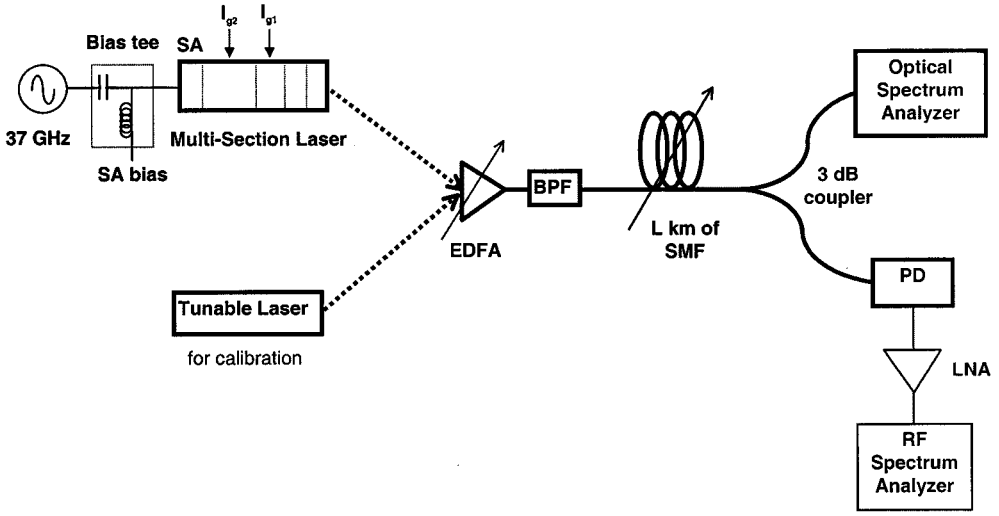

Fig. 6. Experimental setup for measurement of dispersion-induced RF power penalty when transporting the optical signal from the multisection laser over fiber.

The complexity of the dispersion simulation decreases with fewer laser modes, therefore, we investigated the accuracy of a reduced-mode model in predicting the RF dispersion penalty. The six-mode model can be reduced to a five-mode model by neglecting the least significant RF beat component and, likewise, a four-mode model can also be realized. A comparison of the calculated dispersion-induced RF power penalties for a four-mode laser model and a six-mode laser model was carried out. It was found that the effect on accuracy was negligible, with a detected RF power difference of less than 0.4 dB in the four-mode model compared to the six-mode model. Thus, a theoretical model comprising four optical modes in the multisection laser output was used for the accurate estimation of the dispersion penalty in such lasers.

III. Dispersion Characterization of the Multisection Laser

In the previous section, we found that a four-mode laser and dispersion model can accurately estimate the detected RF power of the millimeter-wave repetition frequency from the multisection laser signal after transmission through optical fiber, when the laser optical spectrum is known. It was also shown that chromatic dispersion results in the loss of RF power in the detected millimeter-wave carrier as the fiber length is varied. In order to fully characterize the dispersion effects, it is essential to characterize the dispersion-induced RF power penalty as a function of the multisection laser operating conditions.

As described in Section II, the DBR section of the multisection laser plays an important role in determining the shape of the optical spectrum, which depends on the strength of the DBR region's spectrum-filtering property [20]. Each multisection laser has a slightly different DBR profile that depends on the fabrication process, which, in turn, affects the resulting optical spectrum from the laser. In addition, when current is injected into the DBR section, the optical signal from the multisection laser can be tuned to another center wavelength with small resulting variations in the envelope of the optical spectrum [19]. In the multisection lasers considered here, however, there were no electrical connections to the DBR section of the laser and, therefore, tuning of the optical spectrum from the laser could only be accomplished by using an external optical BPF. In order to quantify the relationship between the optical spectrum from the multisection laser and the resulting dispersion-induced RF power penalties, we emulate the effect of strong DBR spectrum filtering within the laser by placing a narrow-band external filter with a center wavelength of 1545.5- and 0.3-nm bandwidth at the output of the multisection laser. The filtered optical spectrum now consists of four optical modes where the power level in the modes can be varied by changing the dc-bias current to the gain section. We are then able to determine the resulting dispersion effects as a function of laser bias conditions. In addition, we can investigate other factors such as the laser locking condition and beat signal phase noise. These results will provide a guideline to the design of the DBR and gain sections in such a multisection laser in order to obtain reduced dispersion effects when transmitting data at millimeter-wave frequencies using the device.

The experimental setup for characterizing the dispersion effects of the multisection laser is similar to that shown in Fig. 6, with the exception of the narrow-band optical filter added at the output of the multisection laser. Fig. 7 shows the measured dispersion-induced RF power penalty for the case of the laser SA with a short circuit termination and gain currents of $I_{g1} = 42$ mA, and $I_{g2} = 87.5$ mA (the measured optical spectrum is shown as an inset). Also shown in Fig. 7 are the theoretical results obtained from the dispersion model, which show good agreement with the measurements. Maintaining I_{g1} at 42 mA, measurements of dispersion-induced power penalty were then repeated for different values of I_{g2}. The laser optical spectrum corresponding to each bias condition was measured and the recorded optical mode power levels were incorporated into the dispersion model in order to predict the resulting RF power dispersion penalty. As described in Section II, ripple depth is defined as the difference between the maximum and minimum detected RF powers from the multisection laser.

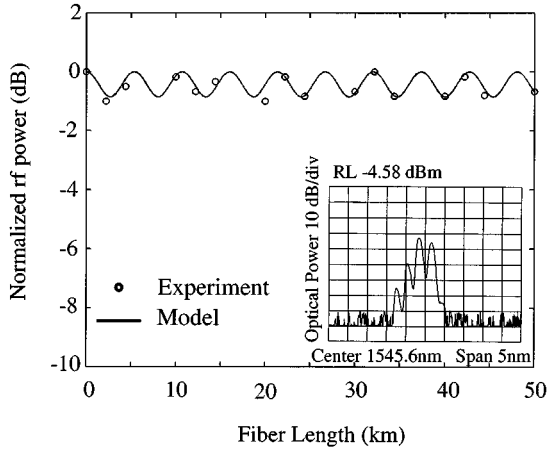

Fig. 7. Measured and predicted dispersion-induced RF power penalty in the multisection laser with strong DBR filtering property and bias currents of $I_{g1} = 42$ mA, $I_{g2} = 87.5$ mA, and a short-circuit at the SA (inset shows the measured optical spectrum at the bias point).

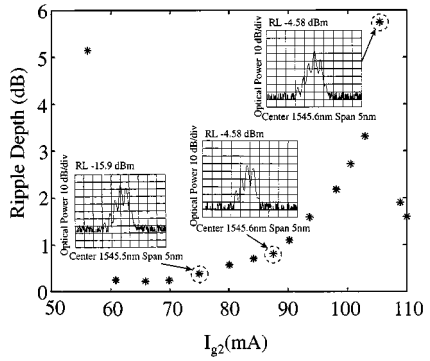

Fig. 8. Dispersion-induced RF power ripple depth as a function of I_{g2} predicted by the dispersion model incorporating the measured optical mode powers when $I_{g1} = 42$ mA with a short circuit at the SA (insets show the measured optical spectra at the indicated bias points).

Figs. 8 and 9 show the dispersion-induced ripple depth plotted as a function of current in the long gain section of the laser (I_{g2}) for the SA with a short- and open-circuit termination, respectively. The insets show the corresponding measured optical spectra at particular operating bias conditions. Figs. 8 and 9 clearly show that the distribution of optical power amongst the modes in the multisection laser spectrum has a significant effect on the resulting dispersion-induced RF power penalty. In particular, maximum cancellation of the detected RF power will occur when the laser optical spectrum is symmetric and similar to that which results in conventional intensity modulation of a single optical carrier (double-sideband modulation). For example, in Fig. 9, this occurs at a gain current of 80 mA where the ripple depth is approximately 50 dB. Figs. 8 and 9 also show that the maximum dispersion-induced RF power penalties occur at different bias points depending on whether the SA is short- or open-circuit terminated. The maximum ripple depth obtained in Fig. 8 is ≈5.8 dB and occurs when the optical modes on either side of the dominant mode exhibit a power difference of approximately 5 dB. However, when these two side modes are almost equal in power (as occurs at $I_{g2} = 80$ mA in Fig. 9), the ripple depth increases dramatically to more than 50 dB. These results

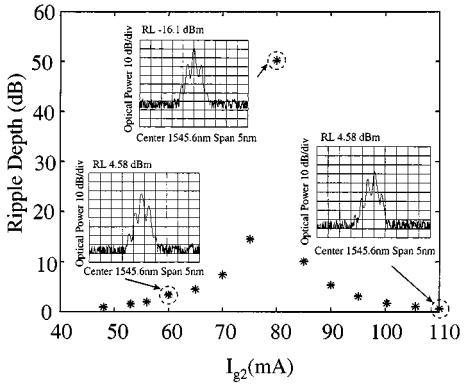

Fig. 9. Dispersion-induced RF power ripple depth as a function of I_{g2} predicted by the dispersion model incorporating the measured optical mode powers when $I_{g1} = 42$ mA with an open circuit at the SA (insets show the measured optical spectra at the indicated bias points).

clearly indicate the sensitivity of the ripple depth to the optical power levels in the laser modes and the significance of the DBR filtering characteristic in shaping the laser spectrum in order to reduce fiber dispersion penalties.

The results obtained in Figs. 8 and 9 enable an optimum operating point to be chosen for the multisection laser in order to achieve minimal dispersion-induced RF power penalties. However, the phase noise and RF power of the resulting beat signal are also important considerations for data transmission using the multisection laser. A detected millimeter-wave signal exhibiting large phase noise degrades the ability to recover the transmitted data and, consequently, the resulting bit error rate (BER). In addition, the maximum detected RF power will affect the signal-to-noise ratio at the millimeter-wave frequency. Section IV investigates these two parameters for the multisection laser.

IV. Detected RF Power and Phase Noise of the Millimeter-Wave Beat Signal From Multisection Laser

In this section, we further investigate the resulting detected RF power and the phase noise of the millimeter-wave beat signal as a function of the laser operating conditions and compare these results with the dispersion-induced power penalties obtained in the previous section. Figs. 10 and 11 show the measured detected RF power of the 37-GHz beat signal from the modulated multisection laser as a function of I_{g2} for the SA with short- and open-circuit terminations, respectively, for $L = 0$ km. Also shown are the calculated RF powers obtained from our theoretical model using the measured power distribution amongst the laser modes. Both sets of results are in good agreement with RF power differences <2.5 dB, which confirms the validity of our model in predicting detected RF powers from the multisection laser.

When the SA of the laser is terminated with a short circuit (Fig. 10), the detected RF power increases with I_{g2} to approximately −50 dBm before decreasing gradually with further increases in gain current. When I_{g2} is 75 mA, as shown in Fig. 8, the optical spectrum exhibits two dominant modes with the other wavelengths at least 18 dB lower in power. The detected beat signal at the receiver will then be dominated by the beating

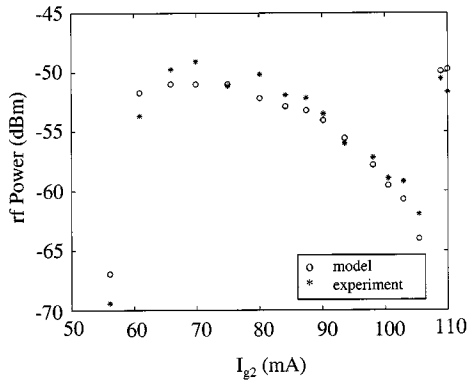

Fig. 10. Measured and calculated RF power of the detected millimeter-wave carrier as a function of I_{g2} when I_{g1} is maintained at 42 mA with a short circuit at the SA.

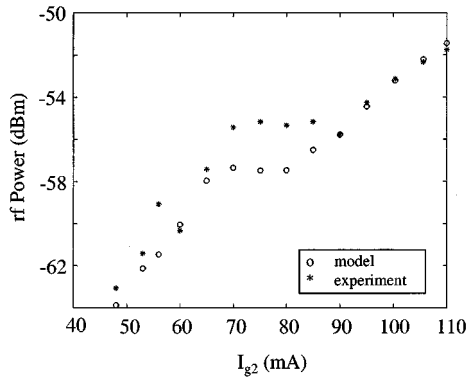

Fig. 11. Measured and calculated RF power of the detected millimeter-wave carrier as a function of I_{g2} when I_{g1} is maintained at 42 mA with an open circuit at the SA.

between the two stronger modes, which results in a larger RF power. As I_{g2} increases gradually, the second largest mode decreases in power and eventually drops to at least 10 dB below the dominant mode (when $I_{g2} = 106$ mA). We expect that the detected RF power in this case will reduce accordingly and Fig. 10 confirms these results. When the SA is terminated with an open circuit (Fig. 11), the RF power increases gradually with I_{g2} initially before decreasing slightly, and then increasing gradually again with I_{g2} to a maximum RF power of approximately -52 dBm. With reference to the optical spectra in the insets of Fig. 9, it is seen that when $I_{g2} = 60$ mA, the side modes are approximately 10 dB below the dominant mode, while the side modes are approximately 18 dB below the dominant mode when $I_{g2} = 80$ mA. However, the detected RF power shows a steady increase within this range of gain currents. This is due to the total average optical power level of the modes when $I_{g2} = 60$ mA being relatively small compared to the average power when $I_{g2} = 70$ mA. The slight reduction in RF power as I_{g2} reaches 80 mA is probably due to the decrease in the optical power of the side mode relative to the dominant mode, which, in turn, causes a decrease in the detected RF power. Further increases in I_{g2} result in an increase in the power level of one of the side modes, which eventually leads to an optical spectrum with two dominant modes. This corresponds to a steady increase

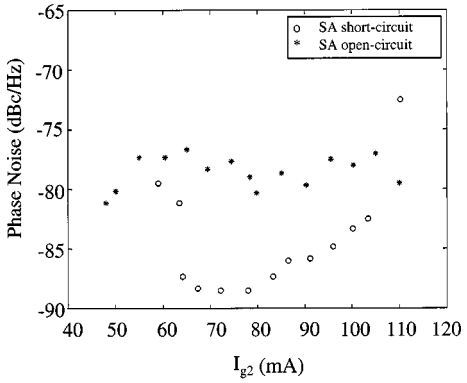

Fig. 12. Measured phase noise at an offset of 100 kHz of the detected millimeter-wave carrier from the multisection laser with a short circuit and open circuit at the SA (injected RF power into the SA $= +4$ dBm).

in the detected RF power, as indicated in Fig. 11. These results for the detected RF power of the 37-GHz signal from the multisection laser clearly correlate closely with the variation of the mode power distribution in the laser optical spectrum.

The phase noise of the detected RF signal at 37 GHz was also measured using the phase-noise utility software of the millimeter-wave spectrum analyzer. In this measurement, the injected RF reference signal into the SA was maintained at $+4$ dBm for all bias current conditions. Fig. 12 shows the measured phase noise of the 37-GHz signal from the laser at an offset frequency of 100 kHz from the carrier, for the SA with short- and open-circuit terminations, as a function of I_{g2} (I_{g1} was maintained at 42 mA). In Fig. 12, the lowest measured phase noise of -88 dBc/Hz is achieved when the SA of the multisection laser is at 0 V with $I_{g2} = 78$ mA. This minimum phase noise indicates that under these operating conditions, the laser is efficiently mode locked by the external reference signal.

From the measurements of the phase noise of the detected 37-GHz beat signal, it is clear that both the detected RF power and phase noise vary significantly with the laser operating conditions. With an open circuit at the laser SA, the ripple depth is minimized for bias currents less than 55 mA and more than 100 mA (Fig. 9). However, the phase noise of the detected RF signal at these operating conditions is large (>-80 dBc/Hz), which indicates that the externally injected RF signal is not strong enough to achieve full locking of the laser. With a short circuit at the SA, a minimum dispersion-induced power penalty is achieved for I_{g2} in the range of 60–80 mA (Fig. 8). At these bias conditions, the phase noise of the detected signal is also a minimum (Fig. 12), while the detected RF power is a maximum (Fig. 10).

The results shown in Section III and Section IV indicate that the optical spectrum of the multisection laser can be tuned so that the laser is tolerant to the effects of fiber chromatic dispersion. However, other parameters such as the detected RF power and the resulting phase noise of the beat signal must also be considered, in order to ensure that the multisection laser is also an efficient source of such signals with maximum signal-to-noise ratio and BER of the recovered data achieved when the laser is used to transmit data. Therefore, the design of the DBR section is crucial in providing the desired spectrum-filtering effect

to produce the optical spectrum, which ensures minimal dispersion penalty and a large detected RF signal with low phase noise.

V. Conclusions

We have developed a simple analytical model to characterize the effect of fiber chromatic dispersion on the transmission of millimeter-wave modulated optical carriers produced by a multisection DBR semiconductor laser. This model is able to predict the dispersion-induced RF power penalty when the output optical spectrum from the multisection laser is known. The effect of dispersion on the transmission of signals from the multisection laser can then be fully characterized and investigated with the developed model. We have also shown that the model exhibits good agreement with experimental measurements of the dispersion-induced RF power penalty. Our investigations have established that the dispersion penalty when using the multisection semiconductor laser to transmit millimeter-wave optical carriers over fiber, strongly depends on the power distribution amongst the optical modes in the laser output. In particular, the dispersion penalty increases dramatically as the laser optical spectrum becomes more symmetrical with one dominant center wavelength. The DBR region of the multisection laser together with the laser gain profile play an important role in determining the laser output spectrum. We have emulated the spectrum-shaping property of the DBR region and have characterized the resulting dispersion-induced RF power penalty of the multisection laser as a function of the laser bias conditions.

In addition to the dispersion-induced RF power penalty, we have also characterized other parameters such as the received RF power and the phase noise of the detected millimeter-wave carrier from the multisection laser. These factors play an important role in determining the quality of the received signals as they affect the resulting carrier-to-noise ratio and BER of the system when the multisection laser is used as a millimeter-wave data transmitter. Our results have shown that the detected RF power and phase noise of the detected millimeter-wave carrier also vary significantly with the laser operating conditions. Therefore, the bias conditions, which give minimum dispersion RF power penalty, do not necessarily provide the best locking conditions for the multisection laser. Consequently, a compromise must be made in obtaining the optimum operating condition for the multisection laser to behave as an efficient millimeter-wave data transmitter, which results in minimum dispersion penalty, maximum detected RF power, and minimum phase noise of the resulting millimeter-wave signals. The results presented in this paper have provided a guideline for designing the DBR section and the gain profile in multisection semiconductor lasers in order to reduce the dispersion-induced RF power penalty on the transmission of the millimeter-wave carrier while ensuring maximum received RF power and minimum phase noise.

Acknowledgment

The authors express their sincere thanks to Dr. Y. Ogawa, OKI Electric Industry Pty. Ltd., Hachioji, Tokyo, Japan, for providing the multisection DBR semiconductor laser used in this paper.

References

[1] H. Ogawa, D. Polifko, and S. Banba, "Millimeter-wave fiber optics systems for personal radio communication," *IEEE Trans. Microwave Theory Tech.*, vol. 40, pp. 2285–2292, Dec. 1992.

[2] J. Park and K. Y. Lau, "Millimeter-wave (39 GHz) fiber-wireless transmission of broadband multichannel compressed digital video," *Electron. Lett.*, vol. 32, no. 5, pp. 474–476, 1995.

[3] G. H. Smith, D. Novak, C. Lim, and K. Wu, "Full-duplex broadband millimeter-wave optical transport system for fiber-wireless access," *Electron. Lett.*, vol. 33, no. 13, pp. 1159–1160, 1997.

[4] J. J. O'Reilly and P. Lane, "Remote delivery of video services using mm-waves and optics," *J. Lightwave Technol.*, vol. 12, pp. 369–375, Feb. 1994.

[5] J. B. Georges, J. Park, O. Solgaard, P. Pepeljugoski, M. Sayed, and K. Y. Lau, "Transmission of 300 Mbps BPSK at 39 GHz using feedforward optical modulation," *Electron. Lett.*, vol. 30, no. 2, pp. 160–161, 1994.

[6] S. Levy, R. Nagarajan, A. Mar, P. Humphrey, and J. E. Bowers, "Fiber-optic PSK subcarrier transmission at 35 GHz using a resonantly enhanced semiconductor laser," *Electron. Lett.*, vol. 28, no. 22, pp. 2103–2104, 1992.

[7] K. Y. Lau and J. B. Georges, "On the characteristics of narrow-band resonant modulation of semiconductor lasers beyond relaxation oscillation frequency," *Appl. Phys. Lett.*, vol. 63, no. 11, pp. 1459–1461, 1993.

[8] J. J. O'Reilly, P. M. Lane, R. Heidemann, and R. Hofstetter, "Optical generation of very narrow linewidth millimeter wave signals," *Electron. Lett.*, vol. 28, no. 25, pp. 2309–2311, 1992.

[9] D. Wake, C. R. Lima, and P. A. Davies, "Optical generation of millimeter-wave signals for fiber-radio systems using a dual-mode DFB semiconductor laser," *IEEE Trans. Microwave Theory Tech.*, vol. 43, pp. 2270–2276, Sept. 1995.

[10] Z. Ahmed, D. Novak, R. B. Waterhouse, and H. F. Liu, "Optically-fed millimeter-wave (37 GHz) transmission system incorporating a hybrid mode-locked semiconductor laser," *Electron. Lett.*, vol. 32, no. 19, pp. 1790–1792, 1996.

[11] C. Lim, D. Novak, and G. H. Smith, "Implementation of an upstream path in a millimeter-wave fiber-wireless system," in *Proc. OFC*, San Jose, CA, 1998, paper Tu3.

[12] G. J. Meslener, "Chromatic dispersion induced distortion of modulated monochromatic light employing direct detection," *IEEE J. Quantum Electron.*, vol. 20, pp. 1208–1216, Oct. 1984.

[13] H. Schmuck, "Comparison of optical millimeter-wave system concepts with regard to chromatic dispersion," *Electron. Lett.*, vol. 31, no. 21, pp. 1848–1849, 1995.

[14] G. H. Smith, D. Novak, and Z. Ahmed, "Overcoming chromatic dispersion effects in fiber-wireless systems incorporating external modulators," *IEEE Trans. Microwave Theory Tech.*, vol. 45, pp. 1410–1415, Aug. 1997.

[15] U. Gliese, S. Nørskov, and T. N. Nielsen, "Chromatic dispersion in fiber-optic microwave and millimeter-wave links," *IEEE Trans. Microwave Theory Tech.*, vol. 44, pp. 1716–1724, Oct. 1996.

[16] S. Arahira, Y. Matsui, and Y. Ogawa, "Mode-locking at very high repetition rates more than terahertz in passively mode-locked distributed-Bragg-reflector laser diodes," *IEEE J. Quantum Electron.*, vol. 32, pp. 1211–1224, July 1996.

[17] D. Y. Kim, M. D. Pelusi, Z. Ahmed, D. Novak, H. F. Liu, and Y. Ogawa, "Ultra-stable millimeter-wave signal generation using hybrid mode-locking of a monolithic DBR laser," *Electron. Lett.*, vol. 31, no. 9, pp. 733–734, 1995.

[18] J. R. Karin, R. J. Helkey, D. J. Derickson, R. Nagarajan, D. S. Allin, J. E. Bowers, and R. L. Thornton, "Ultrafast dynamics in field-enhanced saturable absorbers," *Appl. Phys. Lett.*, vol. 64, no. 6, pp. 676–678, 1994.

[19] H. F. Liu, S. Arahira, T. Kunii, and Y. Ogawa, "Tuning characteristics of monolithic passively mode-locked distributed Bragg reflector semiconductor laser," *IEEE J. Quantum Electron.*, vol. 32, pp. 1965–1975, Nov. 1996.

[20] S. Arahira and Y. Ogawa, "Repetition-frequency tuning of monolithic passively mode-locked semiconductor lasers with integrated extended cavities," *IEEE J. Quantum Electron.*, vol. 33, pp. 255–264, Feb. 1997.

[21] N. P. Caponio, M. Goano, I. Maio, M. Meliga, G. P. Bava, G. Desefanis, and I. Montrosset, "Analysis and design criteria of three-section DBR tunable lasers," *IEEE J. Select. Areas Commun.*, vol. 8, pp. 1203–1212, June 1990.

[22] A. F. Elrefaie, R. E. Wagner, D. A. Atlas, and D. G. Daut, "Chromatic dispersion limitations in coherent lightwave transmission systems," *J. Lightwave Technol.*, vol. 6, pp. 704–709, May 1988.

Christina Lim (S'97–M'00) received the B.E. degree (with first-class honours) in electrical and electronic engineering and the Ph.D. degree from The University of Melbourne, Parkville, Vic., Australia.

Since 1996, she has been with the Photonics Research Laboratory, The University of Melbourne, where she is currently a Research Fellow. Her research interests include fiber-optic wireless communication systems, applications of mode-locked lasers, and optical communication systems.

Dalma Novak (S'90–M'91) received the B.E. degree (with first-class honours) in electrical engineering and the Ph.D. degree from the University of Queensland, Queensland, Queens., Australia, in 1987 and 1992, respectively. Her doctoral dissertation investigated the dynamic behavior of directly modulated semiconductor lasers.

In September 1992, she joined the Photonics Research Laboratory (PRL) [a member of the Australian Photonics Cooperative Research Centre (CRC)], Department of Electrical and Electronic Engineering, The University of Melbourne, Parkville, Vic., Australia, where she is currently an Associate Professor and Reader. She is also a Key Researcher in the CRC, Director of the Melbourne Division of the CRC, and Deputy Director of the PRL. Her research interests include fiber-wireless communication systems, semiconductor lasers, and high-speed optical networks. She has authored or co-authored over 120 papers in these areas.

Prof. Novak is chair of the IEEE Victorian Lasers and Electro-Optics Society (LEOS)/Electron Devices Society (EDS) Chapter and chair of the IEEE Australia Council.

Ampalavanapillai Nirmalathas (M'98) received the B.E. (with honours) and Ph.D. degrees in electrical and electronic engineering from The University of Melbourne, Parkville, Vic., Australia, in 1993 and 1997, respectively.

In 1997, he joined the Photonics Research Laboratory, The University of Melbourne, where he is currently a Senior Research Fellow. His research interests include fiber-optic feed networks for wireless systems, modeling of optical and wireless communication systems, mode-locked lasers, and microwave photonics.

Graham H. Smith (S'91–M'00) received the Bachelor of Engineering degree (with honors), the Master of Engineering Science degrees from the University of Queensland, Queensland, Queens., Australia, in 1991 and 1993, respectively, and the Ph.D. degree from The University of Melbourne, Parkville, Vic., Australia, in 2000.

From 1993 to 1996, he was a Research Engineer with CSIRO Telecommunications and Industrial Physics, Epping, Australia, where he was involved in the area of high electron-mobility transistor (HEMT) modeling, monolithic-microwave integrated-circuit (MMIC) design [computer-aided design (CAD)], MMIC packaging, and millimeter-wave communication systems. In 1996, he joined the Photonics Research Laboratory (PRL), Department of Electrical and Electronic Engineering, The University of Melbourne. In 1999, he began research in the Optical Enterprise Networks Research Group, Bell Laboratories, Lucent Technologies, Holmdel, NJ, where he is currently involved in high-speed Ethernet networks (10 Gb/s), wavelength division multiplexing (WDM), Internet protocal (IP) restoration of networks, and IP/wave division multiplexing (WDM). His research interests include electromagnetics, fiber-radio networks, IP, and GbE and 10 GbE optical networks.